Selected Paper

The β-Sheet Structure pH Dependence of the Core Fragments of β_2-Microglobulin Amyloid Fibrils

Hirotsugu Hiramatsu,[1,†] Ming Lu,[1,††] Yuji Goto,[2] and Teizo Kitagawa*[1,†††]

[1]Okazaki Institute for Integrative Bioscience, National Institutes of Natural Sciences, Okazaki 444-8787

[2]Institute for Protein Research, Osaka University, 3-2 Yamadaoka, Suita, Osaka 565-0871

Received November 30, 2009; E-mail: Riken-kitagawa@mosk.tytlabs.co.jp

Amyloid fibril structures of peptides having the sequence of the #20–41 region of β_2-microglobulin (β_2m_{20-41} and β_2m_{21-29}) were investigated with FTIR microscope spectroscopy. pH dependence of the amide I band of the IR absorption spectra was analyzed. For β_2m_{20-41}, the β-sheet content at pH 6.0 was 55% (12.1 residues) and the β-sheet was located in the N21–G29 and I35–V37 regions, but at pH 2.5 it was 60% (13.1 residues) and located in the F22–V27 and P32–V37 regions. The two structures with different amounts of β-sheet were switched at pH 4.5, which was close to the pI of this sequence (ca. 4.3) rather than the pK_a of the carboxyl groups (5.8 ± 0.3 and 3.3 ± 0.4), suggesting the importance of the total number of charges rather than protonation of specific residue(s). The spectral characteristics of the IR linear dichroism and ^{13}C isotope labeling indicated the formation of parallel β-sheet structure in both regions, and the stacking direction was unaltered by pH change. Unexpectedly however, the IR spectra of the β_2m_{21-29} fibril demonstrated the simultaneous presence of parallel/anti-parallel β-sheets. The relevance of the pH dependence of the β_2m_{20-41} fibril structure to that of β_2m fibrils is discussed.

β_2-Microglobulin (β_2m), the light chain of the class I major histocompatibility complex, is a main component of amyloid fibrils deposited in the synovial membrane of the carpal tunnel.[1,2] The deposition of amyloid fibril of β_2m, an aggregation with a needle-like morphology and one-dimensional periodicity,[3] causes a serious complication in patients on long-term dialysis, and it is known as dialysis-related amyloidosis. The retention of β_2m in the plasma has been considered to be one of the necessary conditions of fibril formation.[4]

In terms of the fibril formation of β_2m under physiological conditions, the contribution of several compounds is supposed to be substantial. For example, the ligation of Cu^{2+} to H31 induces the cis–trans isomerization of P32,[5,6] which removes the β-bulge at D53–L54 and facilitates the intermolecular interaction.[7] Computational analysis suggests that removal of the β-bulge also occurs preferentially upon the protonation of nearby carboxyl groups.[8] Another compound causing fibril formation is collagen fibers;[9] the fibril formation of β_2m is observed on the surface of collagen, and the importance of the positively charged regions on the surface of the fiber is evident.

The influence of certain detergents,[10] fatty acids,[11] and other factors, including ionic additives like salts and protons, have also been reported. The salt concentration and pH conditions affect the fibril morphology,[12–15] in which preferential coordination of metal ions to protein residues, rather than ionic potency, is considered to affect the fibril formation.[15] The concentration of protons (pH) is also important. The fibril formation of β_2m without a seed does not occur above pH 4.6,[12] and the efficiency is highest at pH 2.5.[13] The pH dependence was ascribed to the protonation of side chains. Interestingly, the midpoint pH values of such changes are different from the isoelectric point of β_2m (p$I \approx 6.1$, calculated value). This suggests the importance of the number of charges in a restricted region rather than that in a whole protein. In this regard, examination of the pH dependence of the fibrilization of the core segments is expected to provide essential information on the pH dependent fibril formation of β_2m.

β_2m consists of seven β-strands (strand A–G), which form two β-sheets (ABED and CFG) in the native conformation,[16] in which the β-sheet content is ca. 50%.[17] The β-sheet structure is retained even under acidic conditions,[18,19] while strands A and G in the native state are excluded from the β-sheet core structure of the fibril.[20] The intermolecular interaction essential to fibril formation may occur at the region covered by strands A and G in the native state, which are strands B and F, respectively. Fibril formation always accompanies intermolecular β-sheet formation. Fibrils exhibit a regular and periodical morphology, so the intermolecular interaction is systematic, and presumably certain specific sequences have to take part in the intermolecular β-sheet of the fibril.

From this viewpoint, a sequence substantial to the intermolecular β-sheet formation is the #20–41 region of β_2m [^{20}SNFLNCYVSGFHPSDIEVDLLK^{41}, denoted as β_2m_{20-41}], the former half of which is strand B in the native state.[16] A peptide fragment having this sequence exhibits a propensity to

† Present address: Graduate School of Pharmaceutical Sciences, Tohoku University, Aobayama, Sendai 980-8578

†† Present address: Key Laboratory for Molecular Enzymology and Engineering, the Ministry of Education, Jilin University, Changchun, Jilin 130021, P. R. China

††† Present address: Toyota Physical & Chemical Research Institute, Nagakute, Aichi 480-1192

Published on the web April 29, 2010; doi:10.1246/bcsj.20090317

spontaneous fibril formation as well as a seeding ability for the fibril formation of the whole β_2m.[21,22] Note that spontaneous fibril formation is uncommon, because most of the fragments having the partial sequence of β_2m do not form the fibril by themselves.[23]

In order to unravel the motive force for the formation of intermolecular β-sheets, the pH dependence of the fibril structures of β_2m_{20-41} and β_2m_{21-29} was examined in this study. FTIR microscopic spectroscopy combined with ^{13}C isotope labeling[24–26] was applied for this purpose, and the fibril structure as well as its change were analyzed. Small pH dependence in the β-sheet content and the position of the β-strands in addition to the conservation of the stacking direction were observed, and the relevance to the fibril formation in β_2m is discussed.

Experimental

Sample Preparation. Two peptides, β_2m_{20-41} [^{20}SNFLNCYVSGFHPSDIEVDLLK^{41}] and β_2m_{21-29} [^{21}NFLNCYVSG^{29}], were synthesized at the Center for Analytical Instruments, National Institute for Basic Biology (Okazaki, Japan), purified by HPLC (Develosil ODS-HG-5 column, Nomura chemical, Japan), and stocked as a DMSO solution (25 mg mL^{-1}) at −80 °C. Seven kinds of single ^{13}C-labeled peptides (F22, V27, G29, P32, I35, V37, and L39) of β_2m_{20-41} and four kinds of single ^{13}C-labeled peptides (at F22, L23, V27, and G29) of β_2m_{21-29} were synthesized separately using the corresponding ^{13}C-labeled amino acid monomers (Cambridge Isotope Lab, Cambridge, MA; atomic purity 99%). The molecular weight of the synthesized peptides was checked by mass spectroscopy.

β_2m_{20-41} was dissolved into buffer containing 100 mM NaCl, and 50 mM citrate (pH 2.0–5.0) or 50 mM phosphate (pH 5.5–8.5), and set to 100 μM. The solution was incubated at 37 °C for 10 h, and the fibril was obtained spontaneously. The β_2m_{21-29} fibrils were prepared in the same way. The fibril formation was verified by observing the ThT fluorescence at 485 nm upon excitation at 455 nm.

The HCl form of #1–40 fragment of human amyloid β-protein ($A\beta_{1-40}$) was purchased from Peptide Institute, Inc. (Osaka, Japan). The peptide was dissolved into buffer containing 100 mM NaCl, and 50 mM phosphate (pH 7.5), and adjusted to 50 μM. The preformed amyloid fibril of $A\beta_{1-40}$ was added as a seed (final concentration was 10 μg mL^{-1}). The solution was incubated at 37 °C for 24 h, and the fibril was obtained.

Spectroscopic Measurements. IR spectra were recorded with a microscope FT-IR spectrometer (Thermo Nicolet Avatar 360, microscope; Thermo Nicolet Continuum FT-IR equipped with an MCT detector). A total of 1024 samplings at a spectral resolution of 4 cm^{-1} were measured for each sample. The measurement was executed in H_2O buffer.

The incubated peptide solutions were centrifuged at 16100 × g for 15 min to sediment fibrils. A pellet of fibrils was soaked in buffer and placed between two CaF_2 windows. The IR spectrum was measured on the pelleted particle in wet condition, and the reference was measured for the solvent at a spot close to the pellets. Neither unbound peptides nor buffer salts appeared on the absorption spectrum of the amyloid sample, because they appear in the reference in the same way as in the sample but have been subtracted from the spectra shown. A negative peak of the solvent band due to the HOH bending band may appear at ca. 1640 cm^{-1} in the IR spectrum of the amyloid sample, because the solvent molecules contained in the volume of the solute are removed from the optical path. The spectral depression due to this effect was compensated numerically by adding the IR spectrum of the solvent so that the absorption due to water at around 2200 cm^{-1} could be cancelled completely.

Since good correlation has been established between the secondary structure of the peptide main chain and the peak position of amide I band,[27] peak frequencies of >1660 cm^{-1} for the non-α-non-β (β-turn, loop, β-bulge, etc.) structures, 1660–1640 cm^{-1} for the α-helix and random coil structures, and 1640–1620 cm^{-1} for the β-sheet structures were used to determine the secondary structure. The number of residues contained in each secondary structure was estimated from the ratio of band intensity under the assumption that the absorption intensity is proportional to the number of carbonyl groups contained in the segment. Thus, the secondary structure content of fibrils was estimated from the observed IR intensities.

IR linear dichroism was recorded for an aligned sample of the fibrils. The aligned sample was prepared by centrifugation;[28] some of the fibril pellets formed by the centrifugation possess partial orientation. The dichroism difference spectrum reflects only the aligned portion, because the spectra of the non-aligned portions are cancelled in the difference calculations. Therefore, the discussion of the aligned moiety is qualitatively justified even if the completeness of the alignment is not sufficiently high. Completeness factor, f, of the alignment (i.e., $f = 1$ for the ideally-aligned sample and $f = 0$ for the non-aligned sample), affects the infrared linear dichroism ratio R (29), and they are related to each other through the angle α between the alignment axis and the direction of the transition dipole moment by

$$R(\alpha, f) = \{f\cos^2\alpha + 1/3(1-f)\}/\{1/2f\sin^2\alpha + 1/3(1-f)\} \quad (1)$$

α was defined to be zero for the band appearing with the largest dichroism.

The IR polarization direction in which the amide I band at ca. 1630 cm^{-1} (assigned to the C=O stretching mode of the β-sheet) became the largest was searched first, and then this direction was regarded as the fibril axis of the aligned sample, because the β-strands ran perpendicular to the fibril long axis and the direction of the C=O bond was parallel to it.

Results

The IR spectra of the β_2m_{20-41} amyloid fibrils were measured at every 0.5 pH unit between pH 6.5 (top) and 2.5 (bottom), as shown in panel A of Figure 1, and the second derivative of individual spectra are depicted in panel B. The raw spectra are decomposed into component bands by fitting them with Gaussian functions. In practice, the amide I and II bands in all nine raw spectra in Figure 1A were fitted simultaneously by assuming seven component bands for amide I, three for amide II region and two side chain bands of the carboxyl group at 1720 cm^{-1} and of Tyr at 1519 cm^{-1}, in which peak positions, bands-widths, and area intensities were chosen as fitting parameters. Here, the peaks at a given frequency were

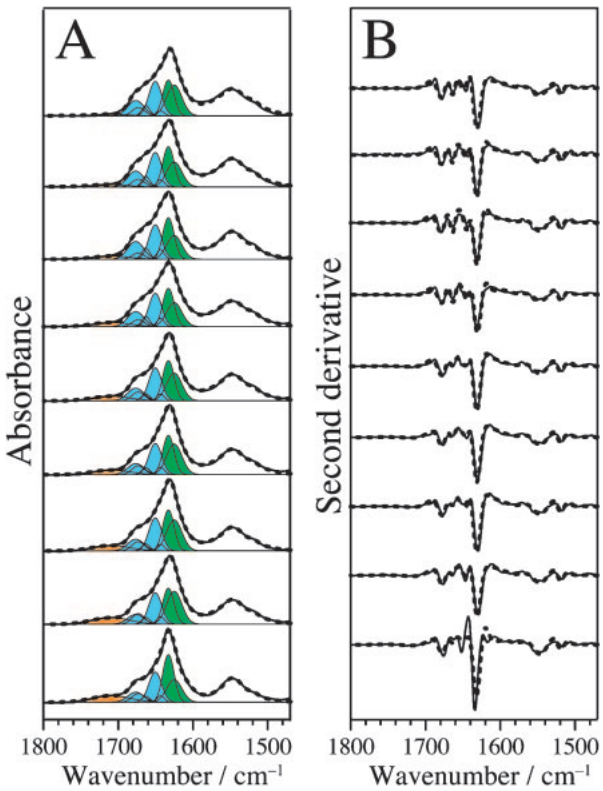

Figure 1. pH dependence of IR spectra of β_2m$_{20-41}$ fibril; Raw absorption spectra in the 1800 to 1470 cm^{-1} region (A, solid lines), their second derivatives (B, solid lines) for the aligned samples at pH 6.5 (top) to pH 2.5 (bottom) with a 0.5 pH interval. The spectra reproduced by fitting analysis are depicted by dotted lines. Component amide I bands obtained from the fitting analysis are colored with green and blue for the β-sheet and the others, respectively, and the C=O stretching band of the COOH group is colored in orange. See the text about the error bars.

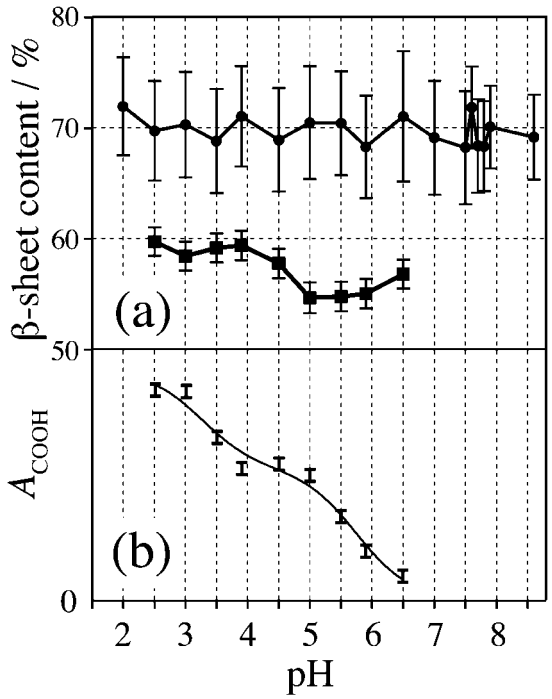

Figure 2. (a) The pH dependence of the β-sheet content of β_2m$_{20-41}$ fibril (square) and of β_2m$_{21-29}$ fibril (circle). (b) The plot of the observed COOH band intensity (bars) and the fitted line (solid line) assuming the presence of the two residues with p$K_a = 5.8$ and one residue with p$K_a = 3.3$.

forced to have a common band-width in the nine spectra. Thus determined seven peak positions and band-widths of amide I are as follows; 1677, 1673, 1663, 1651, 1644, 1633, and 1625 cm^{-1}, and 15, 12, 7, 12, 8, 10, and 14 cm^{-1}. The sum of the component bands of amide I (fitted spectra, dotted lines) successfully reproduced the amide I region of the observed spectra (solid lines in A) and their second derivatives (solid lines in B). Considering the relationship between the secondary structure and the peak position,[27] the component bands at 1633 and 1625 cm^{-1} were assigned to the β-sheet structure (colored green in Figure 1A), and the others were attributed to other structures (colored blue in Figure 1A). The band colored in orange is due to the C=O stretch of protonated carboxyl groups, and the behavior of this band will be discussed later.

The β-sheet content was calculated according to the Lambert–Beer's law from the ratio of the area of the bands assigned to the β-sheet to the total area of the amide I band. The results are plotted in Figure 2a, in which the molar extinction coefficient was assumed to be unaltered by the secondary structures. In Figure 2a, the squares and circles denote the results from β_2m$_{20-41}$ and β_2m$_{21-29}$, respectively. The β_2m$_{20-41}$ fibril seems to exhibit a transition around pH 4.5; the β-sheet content was 12.1 residues (55%) at pH 6.0 and 13.1 residues (60%) at pH 2.5. Certain differences must be present in the fibril structures of β_2m$_{20-41}$ between pH values above and below pH 4.5. It is stressed that the β-sheet content determined for β_2m$_{21-29}$ with the same method did not show such a transition, as plotted by the circles in Figure 2a.

One may argue against the approximation that the molar extinction coefficients are the same among different secondary structures.[29,30] In the limiting case that the coefficient of the β-sheet structure is 1.31 times larger than that of the random structure,[30] the band area analysis would result in the smaller β-sheet content; 10.6 residues (48%) at pH 6.0 and 11.7 residues (53%) at pH 2.5. The numbers are still variable, because the extinction coefficient of the other structure (namely the loop structure, see below) is not given explicitly. The errors in the estimated numbers of residues are mainly derived from the uncertainty of the molar extinction coefficient, which may become a few residues in the present case. This error is larger than the systematic error that was considered to be nearly 5% ($\pm$0.7 residues).[17] The absence of a band at 1680–1690 cm^{-1}, known as the $\nu(0,\pi)$ band of the anti-parallel β-sheet,[31,32] suggests parallel stacking. The validity will be discussed later separately, because the stacking direction is important and should be determined carefully.

To characterize the differences in the two fibril structures obtained below/above pH 4.5, the position of the β-sheet in the sequence was first determined by using ^{13}C isotope labeling.[24,26,33,34] Seven kinds of ^{13}C-labeled peptides (at F22, V27, G29, P32, I35, V37, and L39) were prepared separately, and their fibril structures were examined. The labeling was

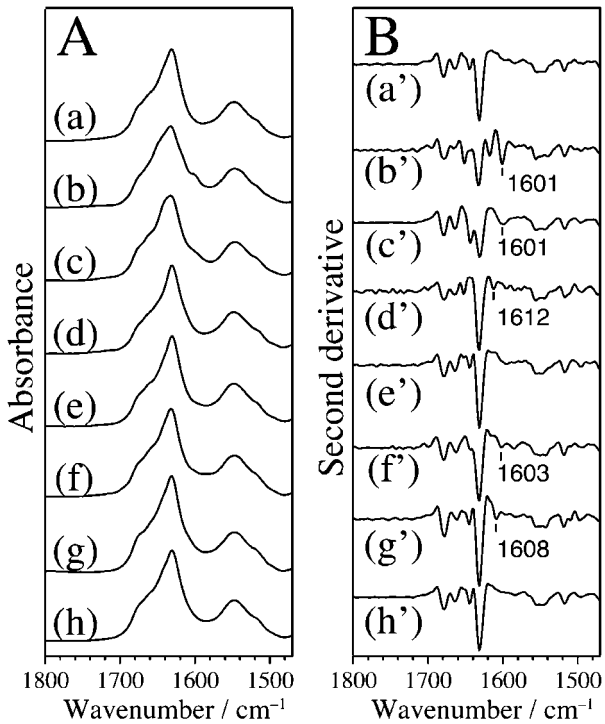

Figure 3. Raw IR spectra (A) and their second derivatives (B) of the β_2m_{20-41} fibril at pH 6.0; non-labeled (a, a′) and ^{13}C-labeled analogs at F22 (b, b′), at V27 (c, c′), at G29 (d, d′), at P32 (e, e′), at I35 (f, f′), at V37 (g, g′), and at L39 (h, h′).

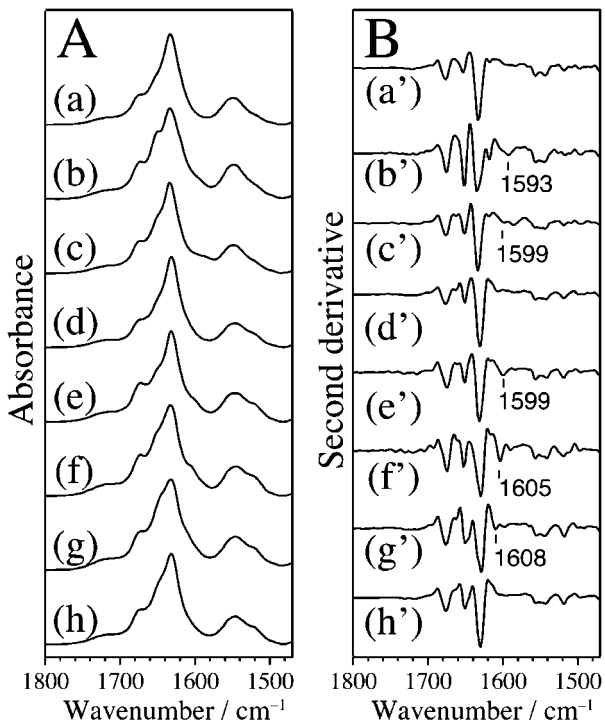

Figure 4. Raw IR spectra (A) and their second derivatives (B) of the β_2m_{20-41} fibril at pH 2.5; non-labeled (a, a′) and ^{13}C-labeled analogs at F22 (b, b′), at V27 (c, c′), at G29 (d, d′), at P32 (e, e′), at I35 (f, f′), at V37 (g, g′), and at L39 (h, h′).

Table 1. Peak Frequencies of the ^{13}C=O Amide I Bands in the Spectra of the β_2m_{20-41} Fibril and the Edge/Middle Assignments[a)]

	Secondary structure contents	
	pH 6.0	pH 2.5
β-Sheet	55% (12.1 residues)	60% (13.1 residues)
Others	45% (8.9 residues)	40% (7.9 residues)
^{13}C=O peak position		
S20		
N21		
F22	1601 cm^{-1}, β[b)], middle	1593 cm^{-1}, β[b)], middle
L23		
N24		
C25		
Y26		
V27	1601 cm^{-1}, β[b)], middle	1599 cm^{-1}, β[b)], edge
S28		
G29	1612 cm^{-1}, β[b)], edge	—[c)], others
F30		
H31		
P32	—[c)], others	1599 cm^{-1}, β[b)], edge
S33		
D34		
I35	1603 cm^{-1}, β[b)], edge	1605 cm^{-1}, β[b)], middle
E36		
V37	1608 cm^{-1}, β[b)], edge	1608 cm^{-1}, β[b)], middle
D38		
L39	—[c)], others	—[c)], others
L40		
K41		

a) Putative location of β-strands is hatched. b) β: β-sheet. c) —: not identified.

performed on the carbonyl carbon atom of the peptide main chain. Figures 3 and 4 show their IR spectra of the fibrils prepared at pH 6.0 and 2.5, respectively, where the observed spectra are depicted in panel A and their second derivatives are in panel B. The observed peak positions of the ^{13}C=O oscillators and the assigned secondary structure of labeled positions are listed in Table 1.

The secondary structures were deduced according to the following criteria, (i)–(iii);

(i) The isotope shift of the ^{13}C=O stretching band of the spatially unfixed residues in a protein (e.g., those in a random coil, loop, etc.) arises mainly from the change of reduced mass. As a consequence, the ^{12}C=O stretching band of these secondary structures at ca. 1660 cm^{-1} becomes weaker and the ^{13}C=O stretching band appears at ca. 1625 cm^{-1}. However, this band is not readily identified in the spectrum of amyloid fibrils, because of the severe overlapping of the ^{12}C=O bands of the β-sheet that appear typically at 1630 cm^{-1}. The electrostatic coupling between the transition dipole moments might be another reason for the peak shift, but relative orientations of the coupled transition dipole moments are not unique in the unfixed part, and accordingly, this term would not be dominant in determining the peak position.

(ii) Because the spatial distributions of the oscillators are fixed in the β-sheet, the transition dipole coupling plays a

significant role in the β-sheet. When each of the β-strands contain a single $^{13}C{=}O$ oscillator, the peak shift is due to both the reduced mass and the transition dipole coupling between the $^{13}C{=}O$ oscillators. The $^{13}C{=}O$ stretching mode of the fibril appears at 1590–1610 cm^{-1} in this case; when the distance between the two $^{13}C{=}O$ oscillators of adjacent molecules is shortened, the coupling effect becomes larger, and the peak position is expected to shift further to lower frequencies.[24] Conversely, the peak shift becomes close to the case of simple mass effect, when the distance between the $^{13}C{=}O$ oscillators becomes large; this is demonstrated with fibrils that consist of different proportions of the $^{12}C{=}O$ and $^{13}C{=}O$ oscillators.[35] Based on this property, the residues in the β-sheet were distinguished from those in other secondary structures.

(iii) The vibrational motions of the oscillators in the random structure are independent from the motion of adjacent oscillators, but those in the β-sheet are not so, because of the strong coupling between the transition dipole moments. It results in the collective motion of the oscillators that is characteristic of the β-sheet. The insertion of the isotope-labeled oscillator affects the collective motion; the magnitude of this effect depends on the location of the labeling. In the case of the parallel β-sheet, the isotope label in the edge does not change the spectral feature largely because the body of the oscillators, and consequently their coupling, remains unchanged. In contrast, the labeling in the middle of the β-sheet weakens the coupling among $^{12}C{=}O$ oscillators, and brings about a comparatively large change in the vibrational mode. Accordingly, the relative magnitude of the observed isotope effect in the $^{12}C{=}O$ stretching band of the β-sheet was exploited for this analysis, and the residue in the middle or edge of the β-sheet was thus diagnosed.

By the criterion (i), P32 and L39 at pH 6.0 and G29 and L39 at pH 2.5 were assigned to the other than β-sheet, because the $^{13}C{=}O$ band was not identified. According to the criterion (ii), F22, V27, G29, I35, and V37 at pH 6.0 and F22, V27, P32, I35, and V37 at pH 2.5 were assigned to the β-strand structure, because the $^{13}C{=}O$ stretching band was detected in the fibrils of the ^{13}C-labeled peptides at each position (Figures 3 and 4 and Table 1). The peak position of the $^{13}C{=}O$ band varied, suggesting that the orientation and/or distance between the $^{13}C{=}O$ oscillators in the β-sheet would not be identical at each position. Then criterion (iii) was considered. Degradation of the band assigned to the β-sheet at 1632 cm^{-1} was outstanding in F22 and V27 at pH 6.0 (Figures 3c′ and 3d′) and in F22, I35, and V37 at pH 2.5 (Figures 4b′, 4f′, and 4g′) in comparison with the others. Also, the band in the 1645–1650 cm^{-1} region was intensified for F22 and V27 at pH 6.0 and F22 at pH 2.5, and the band broadening was observed for I35 and V37 at pH 2.5. Therefore, they were assigned to the middle of the β-sheet. The isotope effect was relatively small in the other residues, and therefore, they were assigned to the edge.

The position of the β-strand in the sequence depends on the pH (Table 1). It was F22–G29 (eight residues) and I35–V37 (three residues) at pH 6.0, while it was F22–V27 (six residues) and P32–V37 (six residues) at pH 2.5. P32 and L39 at pH 6.0 as well as G29 and L39 at pH 2.5 were assigned to the structure other than the β-sheet. As F22 was assigned to the middle part of the β-strand, and moreover, the β-sheet content was 12.1 residues at pH 6.0, the β-strand can be extended to N21–G29 (nine residues). It is noted, however, that nine-residue β-strands are rarely observed in general proteins; β-strands longer than nine residues have been found in only 12.5% of examples to date (714 out of 5698).[36] At pH 2.5, on the other hand, F22–V27 and P32–V37 were assigned to the β-sheet. N21 or D38 was inferred to be in the β-strand, because F22 and V37 were not assigned to the edge of the β-sheet (taking the margin of error into account, it is possible to assign both residues to β-sheet). Thus, the 13.1 residues of the β-strand were divided into two parts, made up of six and seven residues. A strand–loop–strand structure was common to pH 6.0 and 2.5, similar to that in the parent β_2m, in which the β-strands at N21–S28 and E36–K41 are connected by a loop (S29–I35).[16]

The intensity of the C=O stretching band of COOH at 1720 cm^{-1} was also pH-dependent (Figure 1A, orange), indicating the protonation of the Asp and Glu carboxyl side chains.[37] The pK_a of the C-terminal carboxyl groups was supposed to be less than 3[38] and therefore, outside of the range we examined. This band should disappear when the protonated form (–COOH) turns to the deprotonated form ($-COO^-$), and accordingly, the intensity of this band is proportional to the fraction of the protonated form of carboxyl groups. The area intensities of the COOH band are plotted against pH in Figure 2b, where two transition points were observed. Correspondingly, two independent events of protonation (i.e., two pK_a numbers) were assumed in the fitting analysis, and the pK_a were determined to be 5.8 ± 0.3 and 3.3 ± 0.4. These pK_a values do not agree with the transition pK value of β_2m_{20-41} fibril (ca. 4.5). There is a possibility that the intensity of the small COOH band at the tail of the large amide I band can be systematically over- or under-estimated. Although the baseline was corrected in order to compensate this influence (Figure 2b, thin line), the fitting error might be a possible origin of the small fraction at pH 6.0.

At this stage, we reexamined the validity of the assignment of the stacking direction of the β-sheets. A parallel β-sheet structure was expected in the β_2m_{20-41} fibrils, because the $\nu(0,\pi)$ band was absent. Even though this consideration was theoretically reasonable, practically it was often obscure, because the expected intensity of the $\nu(0,\pi)$ band was unclear.

The amyloid fibril of a peptide fragment having the sequence of the #21–29 region of β_2m [^{21}NFLNCYVSG^{29}][39] (denoted as β_2m_{21-29}) is expected to serve as a good material for this determination. Figure 5a shows the raw spectra of this fibril prepared at pH 2.0–8.6. The strong band at ca. 1630 cm^{-1} indicates the β-sheet structure, and the pH dependence was seen in the other part; a band appeared at ca. 1695 cm^{-1} below pH 7.7, while another band appeared at ca. 1640 cm^{-1} above pH 7.9. The pH dependence was quite pronounced. The ca. 1695 cm^{-1} band is not due to the COO^- antisymmetic stretch band of trifluoroacetic acid, because the pH dependence is inconsistent with its pK_a value (p$K_a \approx 0.3$). Judging from the spectral features, the structures above/below pH 7.8 were considered to be parallel/anti-parallel β-sheets, respectively. Similar spectra of the same peptide in which only the terminal charges were blocked (denoted as β_2m_{21-29}R) are shown in Figure 5b. It is apparent that the transformation detected at pH 7.8 for β_2m_{21-29} disappeared when the terminal charges were blocked.

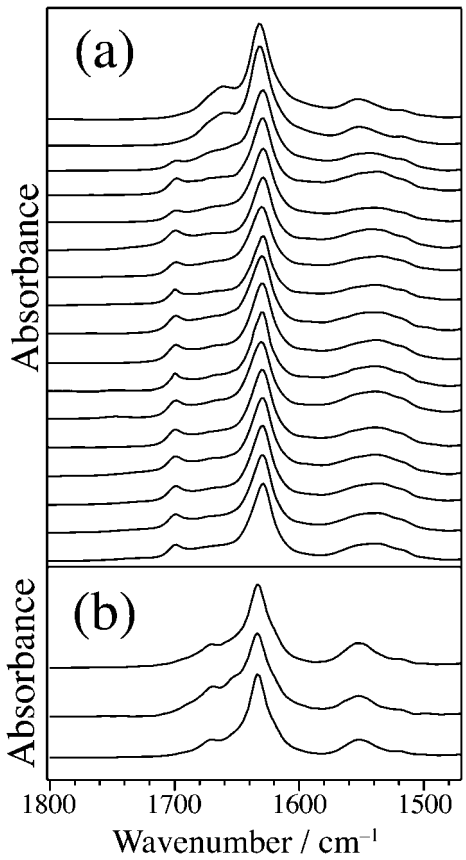

Figure 5. pH dependence of the IR spectrum of the β_2m_{21-29} fibril (a) and β_2m_{21-29}R fibril (b). The spectra in (a) are in the order of pH 8.6 (top), 7.9, 7.8, 7.7, 7.6, 7.5, 7.0, 6.5, 6.0, 5.5, 5.0, 4.5, 3.9, 3.5, 3.0, 2.5, and 2.0 (bottom), and the spectra in (b) were obtained at pH 8.6 (top), 6.0 (middle), and 2.0 (bottom).

In order to confirm the assignment of the stacking direction, IR linear dichroism measurements were performed. The non-polarized IR spectra of β_2m_{21-29} fibrils prepared at pH 7.5 (a) and 8.5 (c) are shown in Figure 6, and the parallel-minus-perpendicular difference spectra of (a) and (c) are depicted in (b) and (d), respectively. A negative peak appeared for the amide II band (ca. 1550 cm^{-1}), because the direction of its transition dipole moment was perpendicular to that of the amide I band at ca. 1630 cm^{-1}. Regarding the $\nu(0,\pi)$ band at ca. 1695 cm^{-1} for which the transition dipole moment should be perpendicular to the $\nu(\pi,0)$ band of the anti-parallel β-sheet at ca. 1630 cm^{-1},[31,32] a negative peak was observed (Figure 6b) as expected. This negative peak was absent in Figure 6d, demonstrating the absence of the $\nu(0,\pi)$ band, and thus the absence of anti-parallel β-sheet. Consequently, spectra (a) and (c) can be regarded as typical examples of anti-parallel and parallel β-sheets of the same peptide. These results are consistent with the present assignment.

For further analysis, the ^{13}C isotope labeling effects on β_2m_{21-29} were separately examined for four residues, F22 (b), L23 (c), V27 (d), and G29 (e) (labeling on the carbonyl carbon atom of the peptide main chain), and the results are shown in Figure 7. The isotope effects on the amide I band were of full variety at pH 6.0 (Figure 7A). This result was ascribed to the

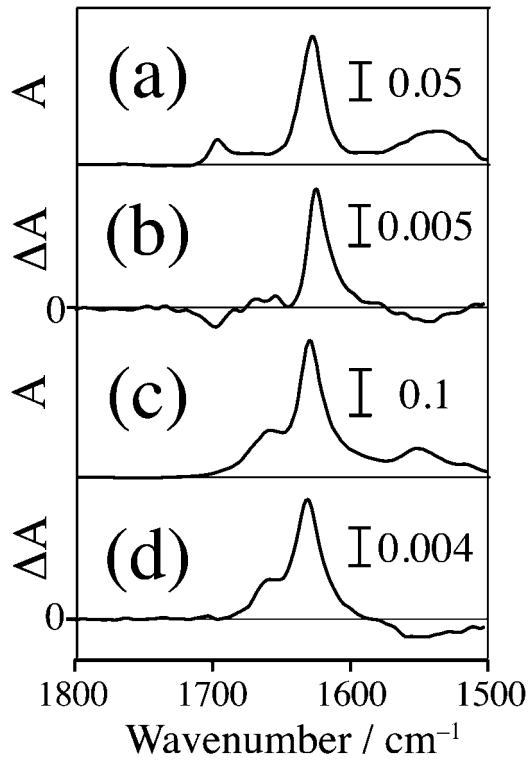

Figure 6. IR absorption spectra of the β_2m_{21-29} fibril prepared at pH 7.5 (a) and 8.5 (c), and the parallel-minus-perpendicular difference spectra from the IR linear dichroism measurements at pH 7.5 (b) and 8.5 (d).

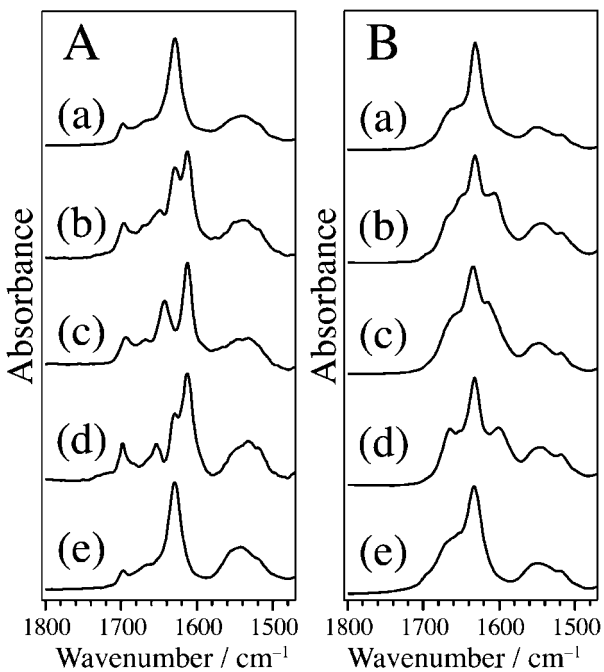

Figure 7. IR spectra of the β_2m_{21-29} fibril at pH 6.0 (A) and pH 8.5 (B); non-labeled (a) and ^{13}C-labeled analogs at F22 (b), L23 (c), V27 (d), and G29 (e).

character of the anti-parallel β-sheet structure in which the distances between the labeled residues in the fibril are varied;[40] for instance, the distance between the F22 residues is different

from that between the L23 residues in the fibril. The intensity of the $^{13}C{=}O$ band was larger than that expected for one-residue substitution out of nine residues (i.e., 1/9 of the amide I band), because this mode picked up intensities from the coupled motions of the $^{12}C{=}O$ oscillators.[34] The isotope effects were observed to be different at pH 8.5 (Figure 7B) from those at pH 6.0; the $^{13}C{=}O$ stretching band appeared as a shoulder of the main peak irrespective of the labeled positions. This indicates that the distances between the $^{13}C{=}O$ oscillators in the F22, the L23, or the V27 substituted fibrils were nearly the same, and these results can be interpreted only with the parallel β-sheet model. Taken together, all the results are consistent with the idea that the β_2m_{21-29} fibril consists of parallel/anti-parallel β-sheet structures in the pH regions above/below pH 7.8. The pH-dependent turnover of the stacking direction in the β_2m_{21-29} fibril was thus demonstrated. The spectral features strongly support the idea that the β_2m_{21-29}R fibril consisted of parallel β-sheets. On the basis of the intensity analysis of the amide I band, the β-sheet content of β_2m_{21-29} was determined to be ca. 70% (6.3 residues out of nine) at all the pH values examined (Figure 2a, circles), and it was deduced from the $^{13}C{=}O$ stretching band that the β-strand was located in F22-V27 (six residues) in the fibril irrespective of the stacking direction.

Based on these results, the spectral features of the β_2m_{20-41} fibril were reexamined and compared with those of the Aβ_{1-40} fibril. Several experimental results indicate the parallel stacking

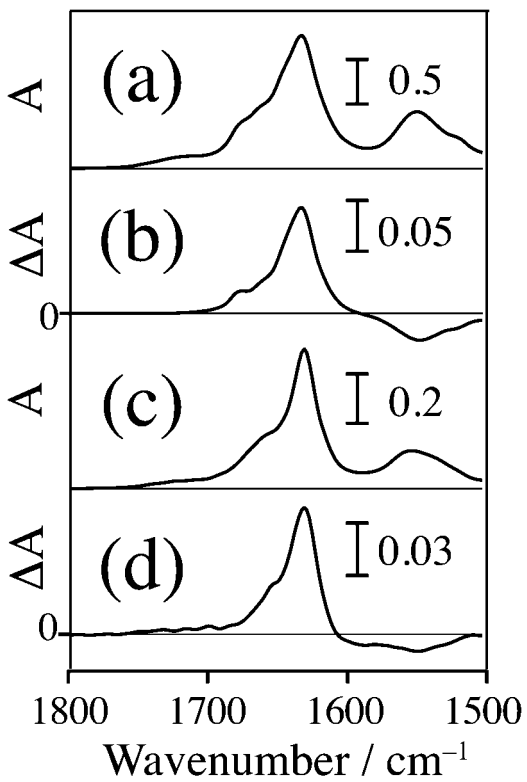

Figure 8. IR absorption spectra of the β_2m_{20-41} fibril prepared at pH 6.0 (a) and of the Aβ_{1-40} fibril prepared at pH 7.5 (c), and the parallel-minus-perpendicular difference spectra from the IR linear dichroism measurements of the β_2m_{20-41} fibril prepared at pH 6.0 (b) and of the Aβ_{1-40} fibril prepared at pH 7.5 (d).

of the β-sheet in the Aβ_{1-40} fibril.[41,42] Figure 8 shows the IR raw spectra of the β_2m_{20-41} fibril prepared at pH 6.0 (a) and the Aβ_{1-40} fibril prepared at pH 7.5 (c), their parallel-minus-perpendicular difference spectra [the β_2m_{20-41} fibril (b) and the Aβ_{1-40} fibril (d)]. If the anti-parallel β-sheet was present in the β_2m_{20-41} fibril, the absorption intensity of the $\nu(0,\pi)$ band would be expected to be ca. 0.8 (=55%/70%) times as large as that at ca. 1695 cm^{-1} of Figure 5a. However, the corresponding band was not recognized in Figures 1 and 8c, and furthermore, the negative peak of the $\nu(0,\pi)$ band, as seen in Figure 6b, was not observed in the IR linear dichroism difference spectrum (Figure 8b). The results from the Aβ_{1-40} fibril are similar to those of the β_2m_{20-41} fibril. In addition, the ^{13}C isotope effects (Figures 3A and 4A) are similar to those of the β_2m_{21-29} fibril at pH 8.5 (Figure 7B). All these results serve as supporting evidence for the presence of parallel β-sheet in the β_2m_{20-41} fibril. The variation of pH affected the structure of β_2m_{20-41} fibril, and the effect appeared in the position of the β-strand in the sequence and also in the β-sheet content, but not in the stacking direction.

Since the amide I band of the β-sheet at 1633 cm^{-1} gave the largest value of $R(\alpha,f)$ (=1.125) in the experiment of the β_2m_{20-41} fibril, f was determined with this band to be 0.04. This means mathematically that only 4% of the fibrils form a domain which are completely aligned to the selected axis and the remaining are random. Practically, however, more fibrils would form the domains but the axes of those domains are distributed and as a result, slightly larger portion of the domains are arranged along the selected axis than to its perpendicular direction. The polarized spectra shown in Figures 6 and 8 try to abstract the structural information on the domains which exhibited the uniaxial arrangement in the statistical sense.

Although the angles α were calculated from the f value and the R values experimentally determined for each band, we do not discuss α values here, as the f value was so low. However, it is noted that the linear dichroism difference spectrum reflects only the aligned part, while non-aligned parts are spectroscopically cancelled and therefore, the qualitative discussion derived from the dichroism observation is justified.

Discussion

The schematic models of the β_2m_{20-41} fibrils at pH 6.0 and 2.5 are delineated in Figures 9a and 9b, respectively. The locations of the β-strands are illustrated with dark and light green arrows (from the N- to C-terminal), and the other parts are colored blue. The structures of the β_2m_{21-29} fibrils at pH 8.6 and 6.0 are depicted in the same manner in Figures 9c and 9d, respectively.

The model of the β_2m_{20-41} fibril at pH 2.5 agrees with the reported structure for the acidic conditions (in a solution containing 10 mM HCl, 1 mM NaCl, and 20% 2,2,2-trifluoroethanol) proposed from the analysis of solid-state NMR spectra, from which the β-strand was allocated to N21–S28 and S33–L40 in the parallel in-register β-sheets.[43] The robustness of the strand–loop–strand structure is also in agreement with a speculation that the β_2m_{20-41} fibrils should have a common structure in the pH range between pH 2.5 and 7.5, because their seeding ability in the fibrilization of β_2m are

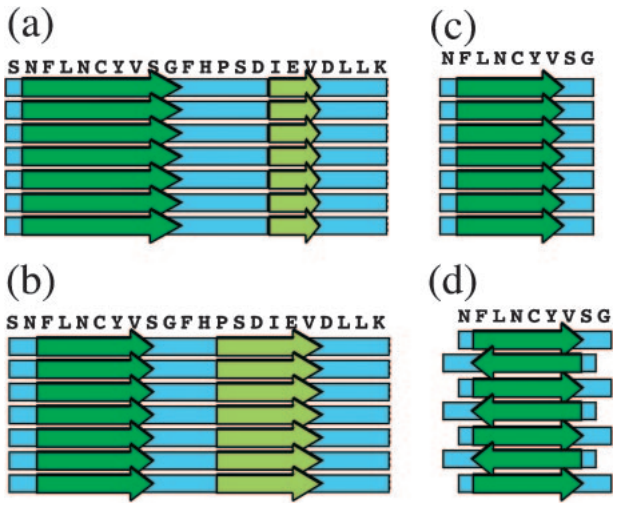

Figure 9. Schematic models of the β_2m_{20-41} fibril at pH 6.0 (a) and pH 2.5 (b), and of the β_2m_{21-29} fibril at pH 8.6 (c) and pH 6.0 (d). Dark and light green colors indicate the positions of the β-strand and the blue ribbon indicates the others. The arrows are in a direction from the N to C-terminal of the segment.

comparable to each other.[22] In addition to β_2m_{20-41},[43] the parallel disposition of the β-strand in amyloid fibrils has been demonstrated for several peptide fragments, e.g., Aβ_{1-40},[41] Aβ_{1-42},[44] the prion domain of Sup35p,[45] Rnq1p,[46] and the N21–H31 fragment of β_2m (β_2m_{21-31}).[25]

A strong band appears at ca. 1630 cm^{-1} in the IR spectra of the β-sheets irrespective of the stacking direction, and this band has been employed as a marker band of the β-sheet structure. Also, a band at ca. 1690 cm^{-1}, referred to as $\nu(0,\pi)$,[31,32] was adopted for diagnosis on the stacking direction (marker for the anti-parallel β-sheet). The criterion has been reached to a consensus with regard to well-ordered models, although not always justified with globular proteins. An objection to the criterion is that proteins containing the parallel β-sheet gave a band above 1675 cm^{-1} in some cases,[42,47,48] and accordingly the assignment of the $\nu(0,\pi)$ band was not straightforward. Furthermore, it was suggested that a distortion (twist) and other factors of the β-sheet make the spectral difference between the parallel and anti-parallel β-sheets less pronounced.[49]

The objections remind us that the amyloid fibril is not a globular protein but is a needle-like aggregate whose length is up to a few μm. Presumably its β-sheet structure is almost infinite, regular, and periodic, and accordingly, the theoretical model[31,32] fits reality more closely in amyloids than in globular proteins. We applied the IR linear dichroism measurement to confirm the assignment of the $\nu(0,\pi)$ band, and in fact, observed the negative band in Figure 6b as theoretically expected. The ^{13}C label location dependence of the isotope shift is also independent evidence for the arrangement. Thus, all the experimental results support the present assignment.

It is worth noting that Brauner et al. proposed the utilization of the ^{13}C labeling for the determination of the stacking direction of the β-strands.[40] They indicated the substantial similarity between the simulated IR spectra of the parallel and anti-parallel β-sheets but clear distinction in the isotope effect. They carried out the simulation for effects of labeling six Gly residues in Aβ_{1-40} on the IR spectra (six-residues labeling for forty-residue peptide). The present results about the β_2m_{21-29} fibril (one-residue labeling for nine-residue peptide) are essentially in agreement with their calculations. That is, the isotope shift appears as a shoulder of the amide I band in the case of parallel β-sheet, but it appears in a different way for anti-parallel β-sheet. Thus, it was shown that isotope labeling in IR spectroscopy has certain potential for the determination of the stacking direction of the β-sheet.

Antzutkin et al. demonstrated parallel stacking of the β-strand in the Aβ_{1-40} fibril with solid-state NMR spectroscopy, and in the same paper they noted that the IR spectrum gave a band assignable to $\nu(0,\pi)$.[42] However, their note is not compatible with our observation; as depicted in Figure 8c, the IR spectrum of the Aβ_{1-40} fibril formed at pH 7.5 in the presence of 100 mM NaCl gave the amide I feature typical of the parallel β-sheet, and the peak position was 1630 cm^{-1}. The linear dichroism (Figure 8d) was also identical to that of the β_2m_{21-29} fibril above pH 7.9 shown in Figure 6d and also to that of β_2m_{20-41} fibril at pH 6.0 shown in Figure 8b. These results are consistent with the Antzutkin's model derived from the solid-state NMR spectroscopy.[42] The peak position of the amide I band they observed (1636 cm^{-1}) seems to be significantly higher than the other cases, for which the anti-parallel β-sheet was concluded.[50–52] In this regard, it is desirable to reexamine their IR spectra.

The β-sheet structure of the F22–V27 region was conserved in the β_2m_{20-41} fibrils at pH 2.5 and 6.0. This region also adopts the β-strand in the native state of β_2m (strand B at N21–S28)[16] and in the denatured state at pH 3.6.[19] This robustness was explained in terms of the high β-sheet-forming propensity associated with the aliphatic and aromatic groups.[53–57] On the other hand, this region was important for the fibril formation of β_2m; strand B (N21–S28) of β_2m was capped by strand A (K6–R12),[16] and exposed to the solvent upon the acid denaturation of strand A.[19] The destabilization of the native state of β_2m occurred below pH 4.7,[12] and correspondingly, the fibril formation took place below pH 4.5.[13] In addition, the elimination of six N-terminal residues (ΔN6–β_2m)[58] facilitated the fibril formation of β_2m. The β_2m_{21-31} fibril induced the fibrilization of the full length β_2m.[35]

The protonation of the carboxyl side chains in the β_2m_{20-41} fibril took place under acidic conditions and the pK_a were determined to be 5.8 ± 0.3 and 3.3 ± 0.4 (Figure 2b), for which two and one carboxyl groups are involved, respectively, judging from the changes of the band intensity. As the pK_a values of carboxyl groups were generally influenced by their local environment,[59] each of the two pK_a might be assigned to a specific side chain. On the other hand, the pK value of the structural change of P32–V37 region (p$K \approx 4.5$) was close to the calculated isoelectric point of β_2m_{20-41} (p$I \approx 4.3$) rather than to the determined pK_a values of carboxyl side chains. Accordingly, it is inferred that the total number of charges is more important than the protonation of specific residue(s).

The pH dependent alteration of the β_2m_{20-41} fibril was observed for the β-strand in the P32–V37 region, which was in contrast with the stability of the β-strand structure of this sequence in β_2m at pH 3.6.[19] The different distributions of the

fibril charges between β_2m and $\beta_2m_{20–41}$ may be responsible. Asp and Glu are scarcely found in the β-strand of the native state of globular proteins,[53] but if present, would hinder the formation of intermolecular β-sheets.[60] Presumably the elimination of electric charges, which would otherwise yield repulsive force, resulted in the emphasized pH dependence of the $\beta_2m_{20–41}$ fibril at pH 2.5. As this pH dependence was ascribed to the properties of the side chains, similar pH dependence was expected for the #20–41 region of the native β_2m. The spontaneous fibril formation of $\beta_2m_{72–99}$ [^{72}PTEKDEYACRVNHVTLSQPKIVKWDRDM^{99}][61] at pH 2.0 might also be explained in terms of the elimination of side chain charges. The apparent pH dependence in the neutral residues (N21, S28, and G29) was considered to be an influence of the whole fibril structure, because the two β-sheets were tightly stacked.[43]

The relevance of this result to the β_2m fibril structure was of interest. To date, two models have been proposed for the intermolecular interactions of proteins in the β_2m fibril, namely head-to-tail and head-to-head structures. One of the former models assumes parallel stacking of the β_2m monomers without the N-terminal (I1–G18) and the C-terminal (W95–M99) residues,[62] in which an intermolecular β-sheet was formed between C25–G29 in strand B and E50–L54 in strand D. In the latter model, a cross-β dimer core consisting of the anti-parallel stacking of strands ABED–DEBA in the β_2m fibril was postulated.[6]

Both models are compatible with our proposed scenario, because they do not include the anti-parallel stacking of the 20–41 region that was excluded by our results. However, we should point out that the intermolecular interaction with strand A in the head-to-head model was unlikely, because of the presence of charged side chains (K6 and R12) which prevent globular proteins from aggregation.[60] The partial denaturation of strand A and the resultant exposure of strand B which occur in this model lead to a different pattern of interaction in the "tail" region; in fact, strand A was not involved in the β-sheet structure of the β_2m fibril.[20] Since the anti-parallel stacking was also excluded by the present results of the $\beta_2m_{21–29}$R fibril, the parallel stacking of strand B is required for this model. In this case, one would suppose that the strand C region cannot be incorporated into the intermolecular β-sheet due to structural limitations of the protein. However, this is against reality, because the strand C region was found in the β-sheet structure in the β_2m fibril.[20] Therefore, the head-to-tail model is more plausible than the head-to-head model to account for the intermolecular interaction, at least as far as the #20–41 region is concerned.

The β-sheet content of the $\beta_2m_{20–41}$ fibril was smaller by one residue at pH 2.5 than at pH 6.0 (Figure 2), and the location of the β-strand was different (Table 1). It is worth mentioning that the proportionality between the length of the β-strand and the stability of the β-sheet structure does not necessarily apply to a long β-strand; this behavior was originally explained in terms of an increase of the α-helix propensity of a sequence upon the increasing growth of strand length.[63] Actually, the incidence of β-strands in proteins decreases steadily as the strands grow longer.[36] Accordingly, the nine-residue β-strand might not result in a stable structure, and the difference in the stability of the $\beta_2m_{20–41}$ fibrils at pH 6.0 and 2.5 could be larger than the value calculated from the difference of the β-sheet content. The stability of the intermolecular β-sheet in the #20–41 region in the β_2m fibril may thus depend on the pH condition. The β-strands with six and seven residues appeared below pH 4.5. The transitional pH value was close to that at which the fibril formation took place.[13] Besides the denaturation,[12] the pH dependence of the property of the segment in the intermolecular β-sheet could be responsible for the fibril formation properties of the protein.

Conclusion

IR spectroscopy combined with ^{13}C isotope labeling enabled us to determine the β-sheet content, the stacking direction, and the secondary structure distribution in the sequence of the $\beta_2m_{20–41}$ fibril. A pH dependence was found for the β-sheet content and the position of the β-strand in the sequence, while not for the stacking direction. Two structures of the $\beta_2m_{20–41}$ fibril were identified; the β-sheet content was 55% and 60% (12.1 and 13.1 out of 22 residues) and the position of the β-strand in the sequence was F22–G29 and I35–V37 at pH 6.0, and F22–V27 and P32–V37 at pH 2.5. The transformation occurred at pH 4.5, which was close to the pI ($\approx$4.3) of the $\beta_2m_{20–41}$ fragment rather than the pK_a of the carboxyl side chains in the #20–41 region. This implies the total number of charges is more important than the protonation state of specific residue(s) in this segment. On the other hand, the $\beta_2m_{21–29}$ fibril was shown to serve as a good example for the simultaneous presence of the parallel and anti-parallel β-sheets in the same segment as it underwent a change in the stacking direction in a pH-dependent manner. This fragment was employed as a model case for determining the IR spectral features of the β-sheets.

The relevance of the present results with the β_2m fibril is as follows. Because of the high propensity of the parallel stacking, as well as the geometric limitations of the protein structure, anti-parallel stacking in the #20–41 region is deemed unlikely. Accordingly, the head-to-tail arrangement was considered to be more plausible than the head-to-head model for the β_2m fibril structure, as far as the #20–41 region is concerned at least. The pH dependent changes in the position of the β-strand in the #20–41 region might be responsible for the pH dependence of the overall stability of the β_2m fibril structure.

This study was supported by JSPS Research Fellowships for Young Scientists to H.H. and by a Grant-in-Aid for Scientific Research (No. 21350098) to T.K from the Japan Society for Promotion of Science. Pacific Edit reviewed the manuscript prior to submission.

References

1 F. Gejyo, T. Yamada, S. Odani, Y. Nakagawa, M. Arakawa, T. Kunitomo, H. Kataoka, M. Suzuki, Y. Hirasawa, T. Shirahama, A. S. Cohen, K. Schmid, *Biochem. Biophys. Res. Commun.* **1985**, *129*, 701.

2 J. M. Campistol, D. Bernard, G. Papastoitsis, M. Solé, J. Kasirsky, M. Skinner, *Kidney Int.* **1996**, *50*, 1262.

3 N. M. Kad, S. L. Myers, D. P. Smith, D. A. Smith, S. E. Radford, N. H. Thomson, *J. Mol. Biol.* **2003**, *330*, 785.

4 F. Gejyo, N. Homma, Y. Suzuki, M. Arakawa, *N. Engl. J. Med.* **1986**, *314*, 585.
5 C. J. Morgan, M. Gelfand, C. Atreya, A. D. Miranker, *J. Mol. Biol.* **2001**, *309*, 339.
6 C. M. Eakin, A. J. Berman, A. D. Miranker, *Nat. Struct. Mol. Biol.* **2006**, *13*, 202.
7 C. H. Trinh, D. P. Smith, A. P. Kalverda, S. E. V. Phillips, S. E. Radford, *Proc. Natl. Acad. Sci. U.S.A.* **2002**, *99*, 9771.
8 S. Park, J. G. Saven, *Protein Sci.* **2006**, *15*, 200.
9 A. Relini, C. Canale, S. D. Stefano, R. Rolandi, S. Giorgetti, M. Stoppini, A. Rossi, F. Fogolari, A. Corazza, G. Esposito, A. Gliozzi, V. Bellotti, *J. Biol. Chem.* **2006**, *281*, 16521.
10 S. Yamamoto, K. Hasegawa, I. Yamaguchi, S. Tsutsumi, J. Kardos, Y. Goto, F. Gejyo, H. Naiki, *Biochemistry* **2004**, *43*, 11075.
11 K. Hasegawa, S. Tsutsumi-Yasuhara, T. Ookoshi, Y. Ohhashi, H. Kimura, N. Takahashi, H. Yoshida, R. Miyazaki, Y. Goto, H. Naiki, *Biochem. J.* **2008**, *416*, 307.
12 V. J. McParland, N. M. Kad, A. P. Kalverda, A. Brown, P. Kirwin-Jones, M. G. Hunter, M. Sunde, S. E. Radford, *Biochemistry* **2000**, *39*, 8735.
13 Y. Ohhashi, Y. Hagihara, G. Kozhukh, M. Hoshino, K. Hasegawa, I. Yamaguchi, H. Naiki, Y. Goto, *J. Biochem.* **2002**, *131*, 45.
14 W. S. Gosal, I. J. Morten, E. W. Hewitt, D. A. Smith, N. H. Thomson, S. E. Radford, *J. Mol. Biol.* **2005**, *351*, 850.
15 B. Raman, E. Chatani, M. Kihara, T. Ban, M. Sakai, K. Hasegawa, H. Naiki, C. M. Rao, Y. Goto, *Biochemistry* **2005**, *44*, 1288.
16 P. J. Bjorkman, M. A. Saper, B. Samraoui, W. S. Bennett, J. L. Strominger, D. C. Wiley, *Nature* **1987**, *329*, 506.
17 A. Dong, P. Huang, W. S. Caughey, *Biochemistry* **1990**, *29*, 3303.
18 H. Katou, T. Kanno, M. Hoshino, Y. Hagihara, H. Tanaka, T. Kawai, K. Hasegawa, H. Naiki, Y. Goto, *Protein Sci.* **2002**, *11*, 2218.
19 V. J. McParland, A. P. Kalverda, S. W. Homans, S. E. Radford, *Nat. Struct. Biol.* **2002**, *9*, 326.
20 M. Hoshino, H. Katou, Y. Hagihara, K. Hasegawa, H. Naiki, Y. Goto, *Nat. Struct. Biol.* **2002**, *9*, 332.
21 G. V. Kozhukh, Y. Hagihara, T. Kawakami, K. Hasegawa, H. Naiki, Y. Goto, *J. Biol. Chem.* **2002**, *277*, 1310.
22 Y. Ohhashi, K. Hasegawa, H. Naiki, Y. Goto, *J. Biol. Chem.* **2004**, *279*, 10814.
23 S. Jones, J. Manning, N. M. Kad, S. E. Radford, *J. Mol. Biol.* **2003**, *325*, 249.
24 C. Paul, J. Wang, W. C. Wimley, R. M. Hochstrasser, P. H. Axelsen, *J. Am. Chem. Soc.* **2004**, *126*, 5843.
25 H. Hiramatsu, Y. Goto, H. Naiki, T. Kitagawa, *J. Am. Chem. Soc.* **2005**, *127*, 7988.
26 S. M. Decatur, *Acc. Chem. Res.* **2006**, *39*, 169.
27 H. Hiramatsu, T. Kitagawa, *Biochim. Biophys. Acta* **2005**, *1753*, 100.
28 H. Hiramatsu, Y. Goto, H. Naiki, T. Kitagawa, *J. Am. Chem. Soc.* **2004**, *126*, 3008.
29 H. H. J. de Jongh, E. Goormaghtigh, J.-M. Ruysschaert, *Anal. Biochem.* **1996**, *242*, 95.
30 M. Jackson, P. I. Haris, D. Chapman, *Biochim. Biophys. Acta* **1989**, *998*, 75.
31 T. Miyazawa, *J. Chem. Phys.* **1960**, *32*, 1647.
32 T. Miyazawa, E. R. Blout, *J. Am. Chem. Soc.* **1961**, *83*, 712.
33 K. J. Halverson, I. Sucholeiki, T. T. Ashburn, P. T. Lansbury, Jr., *J. Am. Chem. Soc.* **1991**, *113*, 6701.
34 J. W. Brauner, C. Dugan, R. Mendelsohn, *J. Am. Chem. Soc.* **2000**, *122*, 677.
35 M. Lu, H. Hiramatsu, Y. Goto, T. Kitagawa, *J. Mol. Biol.* **2006**, *362*, 355.
36 C. Penel, R. G. Morrison, P. D. Dobson, R. J. Mortishire-Smith, A. J. Doig, *Protein Eng.* **2003**, *16*, 957.
37 A. Barth, C. Zscherp, *Q. Rev. Biophys.* **2002**, *35*, 369.
38 D. Voet, J. G. Voet, *Biochemistry*, 2nd ed., John Wiley & Sons, Inc., **1995**.
39 K. Hasegawa, Y. Ohhashi, I. Yamaguchi, N. Takahashi, S. Tsutsumi, Y. Goto, F. Gejyo, H. Naiki, *Biochem. Biophys. Res. Commun.* **2003**, *304*, 101.
40 J. W. Brauner, C. R. Flach, R. Mendelsohn, *J. Am. Chem. Soc.* **2005**, *127*, 100.
41 A. T. Petkova, Y. Ishii, J. J. Balbach, O. N. Antzutkin, R. D. Leapman, F. Delaglio, R. Tycko, *Proc. Natl. Acad. Sci. U.S.A.* **2002**, *99*, 16742.
42 O. N. Antzutkin, J. J. Balbach, R. D. Leapman, N. W. Rizzo, J. Reed, R. Tycko, *Proc. Natl. Acad. Sci. U.S.A.* **2000**, *97*, 13045.
43 K. Iwata, T. Fujiwara, Y. Matsuki, H. Akutsu, S. Takahashi, H. Naiki, Y. Goto, *Proc. Natl. Acad. Sci. U.S.A.* **2006**, *103*, 18119.
44 T. Lührs, C. Ritter, M. Adrian, D. Riek-Loher, B. Bohrmann, H. Döbeli, D. Schubert, R. Riek, *Proc. Natl. Acad. Sci. U.S.A.* **2005**, *102*, 17342.
45 F. Shewmaker, R. B. Wickner, R. Tycko, *Proc. Natl. Acad. Sci. U.S.A.* **2006**, *103*, 19754.
46 R. B. Wickner, F. Dyda, R. Tycko, *Proc. Natl. Acad. Sci. U.S.A.* **2008**, *105*, 2403.
47 R. Khurana, A. L. Fink, *Biophys. J.* **2000**, *78*, 994.
48 H. Susi, D. M. Byler, *Arch. Biochem. Biophys.* **1987**, *258*, 465.
49 J. Kubelka, T. A. Keiderling, *J. Am. Chem. Soc.* **2001**, *123*, 12048.
50 K. Halverson, P. E. Fraser, D. A. Kirschner, P. T. Lansbury, Jr., *Biochemistry* **1990**, *29*, 2639.
51 P. T. Lansbury, Jr., *Biochemistry* **1992**, *31*, 6865.
52 P. E. Fraser, D. R. McLachlan, W. K. Surewicz, C. A. Mizzen, A. D. Snow, J. T. Nguyen, D. A. Kirschner, *J. Mol. Biol.* **1994**, *244*, 64.
53 P. Y. Chou, G. D. Fasman, *Annu. Rev. Biochem.* **1978**, *47*, 251.
54 C. K. Smith, L. Regan, *Science* **1995**, *270*, 980.
55 C. K. Smith, L. Regan, *Acc. Chem. Res.* **1997**, *30*, 153.
56 S. E. Kiehna, M. L. Waters, *Protein Sci.* **2003**, *12*, 2657.
57 M. Reches, E. Gazit, *Science* **2003**, *300*, 625.
58 G. Esposito, R. Michelutti, G. Verdone, P. Viglino, H. Hern ÁNdez, C. V. Robinson, A. Amoresano, F. Dal Piaz, M. Monti, P. Pucci, P. Mangione, M. Stoppini, G. Merlini, G. Ferri, V. Bellotti, *Protein Sci.* **2000**, *9*, 831.
59 W. R. Forsyth, J. M. Antosiewicz, A. D. Robertson, *Proteins* **2002**, *48*, 388.
60 J. S. Richardson, D. C. Richardson, *Proc. Natl. Acad. Sci. U.S.A.* **2002**, *99*, 2754.
61 M. I. Ivanova, M. Gingery, L. J. Whitson, D. Eisenberg, *Biochemistry* **2003**, *42*, 13536.
62 H. Benyamini, K. Gunasekaran, H. Wolfson, R. Nussinov, *J. Mol. Biol.* **2003**, *330*, 159.
63 H. E. Stanger, F. A. Syud, J. F. Espinosa, I. Giriat, T. Muir, S. H. Gellman, *Proc. Natl. Acad. Sci. U.S.A.* **2001**, *98*, 12015.